

## Superconductivity of graphite intercalation compounds with alkali-metal amalgams

Yasuhiro Iye and Sei-ichi Tanuma

*The Institute for Solid State Physics, The University of Tokyo, Roppongi, Minato-ku, Tokyo 106 Japan*

(Received 10 November 1981)

Superconductivity of the alkali-metal amalgam graphite intercalation compounds of stage 1 ( $C_4K\text{Hg}$ ,  $C_4\text{RbHg}$ ) and stage 2 ( $C_8K\text{Hg}$ ,  $C_8\text{RbHg}$ ) has been studied as well as that of the pristine amalgams ( $K\text{Hg}$ ,  $\text{RbHg}$ ). The transition temperatures are 0.73, 0.99, 1.90, and 1.40 K for  $C_4K\text{Hg}$ ,  $C_4\text{RbHg}$ ,  $C_8K\text{Hg}$ , and  $C_8\text{RbHg}$ , respectively. The critical-field anisotropy ratio  $H_{c2}^{\perp}/H_{c2}^{\parallel}$  is about 10 for the stage 1 and about 15 to 40 for the stage 2. It is argued that electrons in the intercalant bands rather than the graphitic bands play the main role in the superconductivity. An interesting feature is that the stage-2 compound, which has a lower density of states at the Fermi level, has a higher transition temperature than the corresponding stage-1 compound.

### INTRODUCTION

Synthetic metals have been one of the major subjects of solid-state physicists in recent years. Among the many interesting physical properties of the new materials, superconductivity has always been of the greatest interest. It was in fact an expectation for high  $T_c$  superconductors that made the earlier researcher in this field enthusiastic. Superconductivity of synthetic metals is also of great theoretical interest in connection with the problem of superconductivity and dimensionality, because most of them have a quasi-one or quasi-two-dimensional character.

For the study of dimensionality and superconductivity, graphite intercalation compounds (GIC's) are especially convenient because of their stage structure; namely, they have such a regular structure that the intercalant layers occupy every  $n$ th inter-carbon-layer spacing. If superconductivity could be observed in several stages of one intercalant species, we would have an ideal system for studying the superconductivity with variable interlayer couplings.

Among graphite intercalation compounds, superconductivity was first found by Hannay *et al.*<sup>1</sup> as early as 1965 in stage-1 alkali-metal GIC's, i.e.,  $C_8\text{K}$ ,  $C_8\text{Rb}$ , and  $C_8\text{Cs}$ . The transition temperatures they reported were  $0.39 \leq T_c \leq 0.55$  K for  $C_8\text{K}$ ,  $0.023 \leq T_c \leq 0.150$  K for  $C_8\text{Rb}$ , and  $0.030 \leq T_c \leq 0.135$  K for  $C_8\text{Cs}$ . Unfortunately, their report could not be confirmed by other researchers. For example, Poitrenaud<sup>2</sup> obtained a negative result as regards the superconductivity of

$C_8\text{K}$  down to 0.30 K.

The superconductivity of  $C_8\text{K}$  was recently confirmed and studied in detail by Koike *et al.*<sup>3</sup> and by Kobayashi *et al.*<sup>4</sup> at lower temperatures. Koike *et al.*<sup>3</sup> investigated 13 samples of  $C_8\text{K}$  synthesized from highly oriented pyrolytic graphite (HOPG) to find transition temperatures ranging from 0.128 to 0.198 K. Kobayashi *et al.*<sup>4</sup> found  $T_c$  of 0.080 K for a sample made from graphite powder and 0.125 K for a sample based on grafoil. As for  $C_8\text{Rb}$  and  $C_8\text{Cs}$ , recent measurements have given negative results down to 0.09 K for  $C_8\text{Rb}$  (Ref. 5) and to 0.06 K for  $C_8\text{Cs}$  (Ref. 6). Superconductivity has not been observed in  $C_6\text{Li}$  or stage-2 alkali-metal GIC's.<sup>5</sup>

More recently, new superconductive GIC's were found. Alexander *et al.*<sup>7</sup> observed an anomaly in the low-temperature specific heat of stage-2 potassium-amalgam GIC,  $C_8K\text{Hg}$  at 1.93 K, which was indicative of the onset of superconductivity. The superconductivity of  $C_8K\text{Hg}$  was subsequently confirmed by Tanuma and Koike<sup>8</sup> and Pendry *et al.*<sup>9</sup> through the observation of the Meissner effect. Pendry *et al.*<sup>9</sup> and Alexander *et al.*<sup>10</sup> also found a superconducting transition in the stage-2 rubidium amalgam GIC,  $C_8\text{RbHg}$ , at 1.44 K.

While it was reported in these stage-2 compounds, superconductivity has not so far been observed in the corresponding stage-1 compounds down to 1.1 K. This was very puzzling because stage-1 compounds have a much higher density of state at the Fermi level and accordingly are expected to be more favorable for superconductivity.

We report here the first observation of supercon-

ducting transitions in stage-1, alkali-metal—amalgam GIC's,  $C_4K\text{Hg}$  and  $C_4\text{RbHg}$ . We also observed the superconducting transitions in the stage-2 compounds, at temperatures consistent with the previous reports.<sup>7–10</sup> We have studied the temperature and magnetic field dependence of superconductivity of these four compounds. The focus of our study is on the critical field anisotropy of these layered superconductors, which will be discussed in comparison with  $C_8K$  (Ref. 3) and other layered superconductors.

We also measured the superconductivity of the pristine materials, i.e.,  $K\text{Hg}$  and  $\text{RbHg}$ , which gave useful information on the nature of the superconductivity of amalgam GIC's.

## II. EXPERIMENTAL

### A. Synthesis and characterization of samples

Alkali-amalgam GIC's were first synthesized by Lagrange *et al.*<sup>11</sup> They have a crystal structure such that the intercalant layer consists of an alkali-mercury-alkali triple layer as shown in the uppermost panel of Fig. 1. The sandwich thickness is 10.15 Å for potassium-amalgam compounds and 10.76 Å for rubidium-amalgam compounds. The in-plane structure of alkali-metal ions is the same as that of  $C_8K$ .

The synthesis of the present samples was done by the same method as Ref. 11. Highly oriented pyrolytic graphite (HOPG) was used as the host graphite. The synthesis of the stage-1 potassium-amalgam GIC  $C_4K\text{Hg}$  was done as follows. Potassium-amalgam  $K\text{Hg}$  was first prepared by reacting a one-to-one molar ratio of distillation-purified potassium and mercury in a sealed glass tube at 260°C for one day. The amalgam was transferred to a new tube together with HOPG chips, which was sealed after evacuation. The intercalation reaction was done at 200°C for several days. Formation of the stage-1 compound  $C_4K\text{Hg}$  was readily recognized by the appearance of a copper-pink luster.

For the stage-2 compound,  $C_8K\text{Hg}$ , two different methods of synthesis are reported. One is to react graphite with a presynthesized one-to-two molar ratio amalgam  $K\text{Hg}_2$  at ca. 300°C. Koike and Tanuma<sup>8</sup> used this method in preparing their sample for superconductivity measurements. The other which we employed in the present work is as follows. First, stage-1 potassium GIC  $C_8K$  was

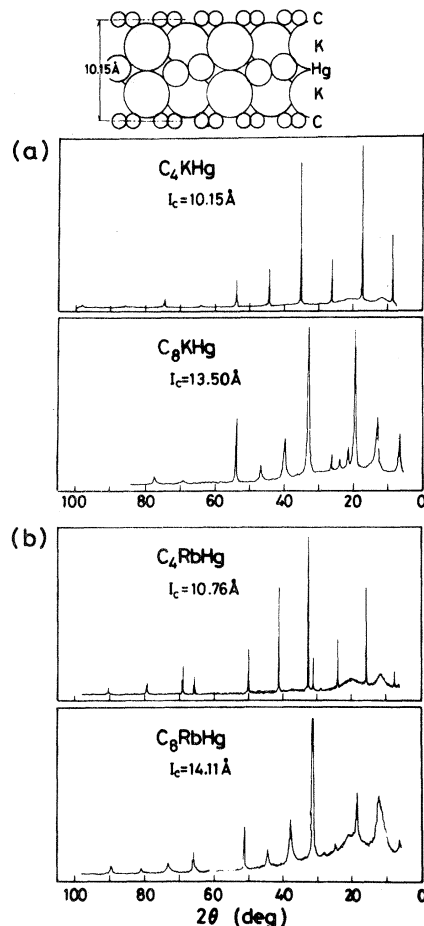


FIG. 1. (00) x-ray diffraction patterns of (a)  $C_4K\text{Hg}$  and  $C_8K\text{Hg}$  and (b)  $C_4\text{RbHg}$  and  $C_8\text{RbHg}$ . The uppermost panel shows the structure of the intercalant layer. The broad peaks around 12° and 20° are due to a plastic sheet used for covering the sample to avoid direct contact with air.

synthesized by the usual vapor-phase reaction. The  $C_8K$  sample was then sealed in a new tube with the stoichiometrically required amount of Hg. The reaction of  $C_8K$  with Hg was witnessed by the change in color of the sample from brass yellow of  $C_8K$  to steel blue of  $C_8K\text{Hg}$ , and the reaction was completed in several hours at 100°C. The samples of Alexander *et al.*<sup>7,10</sup> and Pendry *et al.*<sup>9</sup> were also prepared by this method.

Synthesis of rubidium-amalgam GIC's,  $C_4\text{RbHg}$  and  $C_8\text{RbHg}$ , were done in the same way as above except that slightly lower reaction temperatures were employed. It should be also mentioned here that our attempt to synthesize sodium-amalgam GIC's or cesium-amalgam GIC's following the same recipe was unsuccessful. The failure of the

latter is interesting in view of the fact that  $C_8Cs$  is in many respects similar to  $C_8K$  and  $C_8Rb$ .

Since all the intermediate products as well as the final products were air-sensitive, their handling was done in a glove box, which was first evacuated by an oil diffusion pump and then filled with helium gas passed through a cold trap at 77 K.

The samples were characterized by (001) x-ray diffraction patterns, of which examples are shown in Fig. 1. Stage-1 samples show sharp diffraction peaks indicating uniform crystal structure. The x-ray patterns of stage-2 samples are less sharp. This is probably related with the method of synthesis. When  $C_8KHg$  is produced by the intercalation of Hg into  $C_8K$ , potassium atoms must rearrange themselves to form the K-Hg-K sandwich on

one hand and the de-intercalated inter-carbon-layer spacing on the other. If a certain number of potassium atoms are trapped at defects and remain as an island of single potassium layer, this will give rise to a disorder in the  $c$ -axis period of  $C_8KHg$ , and hence a broadening of the x-ray peaks. The samples were x-rayed immediately after the superconductivity measurements and no degradation in staging was found.

### B. Measurement

The experimental procedure was as follows. A sample was taken out of the reaction tube in the glove box, and wrapped with Parafilm (American Can Co.). The sample was then taken out of the glove box, quickly mounted on a cryostat, and cooled. During this procedure, the wrapping with Parafilm protected the air-sensitive sample reasonably well.

A  $^3He$  evaporation refrigerator was used to attain low temperatures down to 0.40 K. Temperature was measured by a carbon resistance thermometer calibrated against  $^3He$  saturated vapor pressure.

The superconducting transition was detected by measuring the ac susceptibility by the conventional modulation technique. The frequency of the modulation field was 27 Hz and the amplitude was ca. 0.2 Oe. The super-normal transition was investigated in various field orientations with respect to the  $c$  axis.

## III. RESULTS

### A. Signal

Figure 2 shows typical recorder traces of super-normal transitions under a magnetic field applied parallel or perpendicular to the  $c$  axis. In contrast to the case of  $C_8K$  reported by Koike *et al.*,<sup>3</sup> we did not observe supercooling effects for any field orientation. We thus conclude that alkali-metal-amalgam GIC's are type-II superconductors in all field orientations.

The observed critical field is then identified with the upper critical field  $H_{c2}$ . The values of  $H_{c2}$  were defined by the intercept of a straight line drawn tangent to the linear region of the susceptibility curve, with the line showing the normal state level, as shown in Fig. 2.

In the case of stage-1 compounds this definition

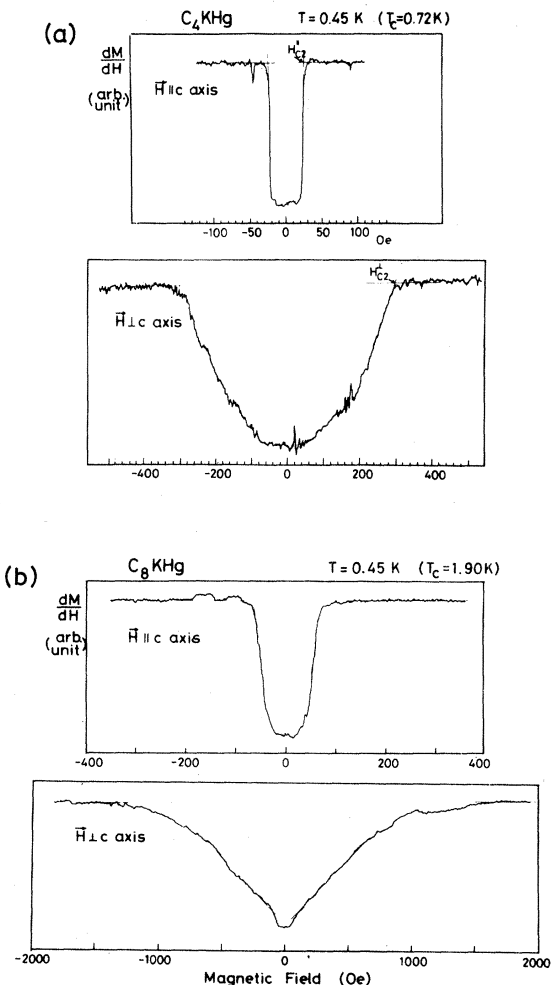


FIG. 2. Recorder traces showing the susceptibility of (a)  $C_4KHg$  (no. 1), (b)  $C_8KHg$  (no. 4) vs the dc magnetic field applied parallel (the upper figures) or perpendicular (the lower figures) to the  $c$  axis.

was fairly obvious. On the other hand, the susceptibility curves of stage-2 compounds in the perpendicular field geometry were such that they made the definition of  $H_{c2}$  less clear and somewhat arbitrary. Although the absolute values of the anisotropy ratio or coherence length discussed in the next section are subject to this arbitrariness, the main conclusions of this paper are insensitive to the choice of the definition of  $H_{c2}$ .

### B. Angular dependence of critical field

In the case of a layered superconductor, one of the simplest models which can be used to explain the anisotropy of  $H_{c2}$  is to assume an elliptical fluxoid.<sup>12</sup> The Ginzburg-Landau (GL) theory for type-II superconductors<sup>13</sup> gives the following expression relating  $H_{c2}$  to the fluxoid:

$$H_{c2} = \frac{\phi_0}{2\pi\xi_\alpha\xi_\beta}, \quad (1)$$

where  $\phi_0$  is the flux quantum and  $\xi_\alpha$  and  $\xi_\beta$  are the two principal coherence lengths in the plane perpendicular to  $H$ . For a layered superconductor, the coherence length is assumed to be isotropic within the layer plane ( $\xi_a = \xi_b = \xi$ ), but for the  $c$  axis it takes a different value ( $\xi_c = \epsilon\xi$ ). Under a magnetic field parallel to the  $c$  axis, the fluxoid is circular in cross section, while for other field orientations it is elliptical. This elliptical fluxoid model with  $H_{c2}$  given by Eq. (1) results in the following expressions for the angular dependence of  $H_{c2}$ :

$$\begin{aligned} H_{c2}(\theta) &= \frac{\phi_0}{2\pi\xi^2} \frac{1}{(\cos^2\theta + \epsilon^2\sin^2\theta)^{1/2}} \\ &= H_{c2}^{\parallel} \frac{1}{(\cos^2\theta + \epsilon^2\sin^2\theta)^{1/2}}, \end{aligned} \quad (2)$$

where  $\theta$  is the angle between  $H$  and the  $c$  axis.<sup>14</sup> In this model, the coherence lengths are assumed to be much larger than the layer spacing. When the coherence length in the  $c$  direction is of the order of the layer spacing, the validity of the model may be questionable.

As seen in Eq. (2), the critical quantity determining the  $H_{c2}$  anisotropy is the ratio of the coherence length in the layer plane to that in the  $c$  direction. This ratio is related by the following expression to the ratio of the effective masses which describe the electron conduction parallel ( $m_a$ ) and perpendicular ( $m_c$ ) to the layer:

$$\epsilon = \frac{\xi_c}{\xi_a} = \left[ \frac{m_a}{m_c} \right]^{1/2}. \quad (3)$$

In this sense, the above model for anisotropic  $H_{c2}$  is often called the effective-mass model. The anisotropic effective mass introduced here is a generalized one and can include contributions from the band effective-mass anisotropy as well as anisotropy in the electron-phonon interaction.

Figure 3 shows the dependence of  $H_{c2}$  of the amalgam GIC's on the field angle with respect to the  $c$  axis. The solid curve in Fig. 3 shows fittings of the angular dependence given by Eq. (2) to the experimental data (points). It is obvious that the angular dependence of  $H_{c2}$  is well explained by the effective-mass model.

### C. Temperature dependence of the critical field

Temperature dependence of the coherence length is given by

$$\xi(T) = \xi(0) \left[ 1 - \frac{T}{T_c} \right]^{-1/2}, \quad (4)$$

in the GL region ( $T_c - T \ll T_c$ ). Substituting Eq. (4) into Eq. (2), we obtain the following expressions for the temperature dependence of the parallel and the perpendicular fields:

$$\begin{aligned} H_{c2}^{\parallel} &= \frac{\phi_0}{2\pi\xi^2(0)} \left[ 1 - \frac{T}{T_c} \right] \\ &= -T_c \left[ \frac{dH_{c2}^{\parallel}}{dT} \right]_{T=T_c} \left[ 1 - \frac{T}{T_c} \right], \end{aligned} \quad (5)$$

$$\begin{aligned} H_{c2}^{\perp} &= \frac{\phi_0}{2\pi\epsilon\xi^2(0)} \left[ 1 - \frac{T}{T_c} \right] \\ &= -T_c \left[ \frac{dH_{c2}^{\perp}}{dT} \right]_{T=T_c} \left[ 1 - \frac{T}{T_c} \right]. \end{aligned} \quad (6)$$

Figure 4 shows the observed temperature dependence of  $H_{c2}^{\parallel}$  and  $H_{c2}^{\perp}$ . In most cases, the perpendicular critical field shows a superlinear temperature dependence (so-called positive curvature) at sufficiently low temperatures. Such positive curvatures are also reported in the case of  $C_8K$  (Ref. 3) and  $2H-NbSe_2$  (Ref. 15) and others, and seem to be a fairly common characteristic of layered superconductors.

Also shown in Fig. 4 is the temperature dependence of  $H_{c2}$  of the pristine amalgams  $KHg$  and

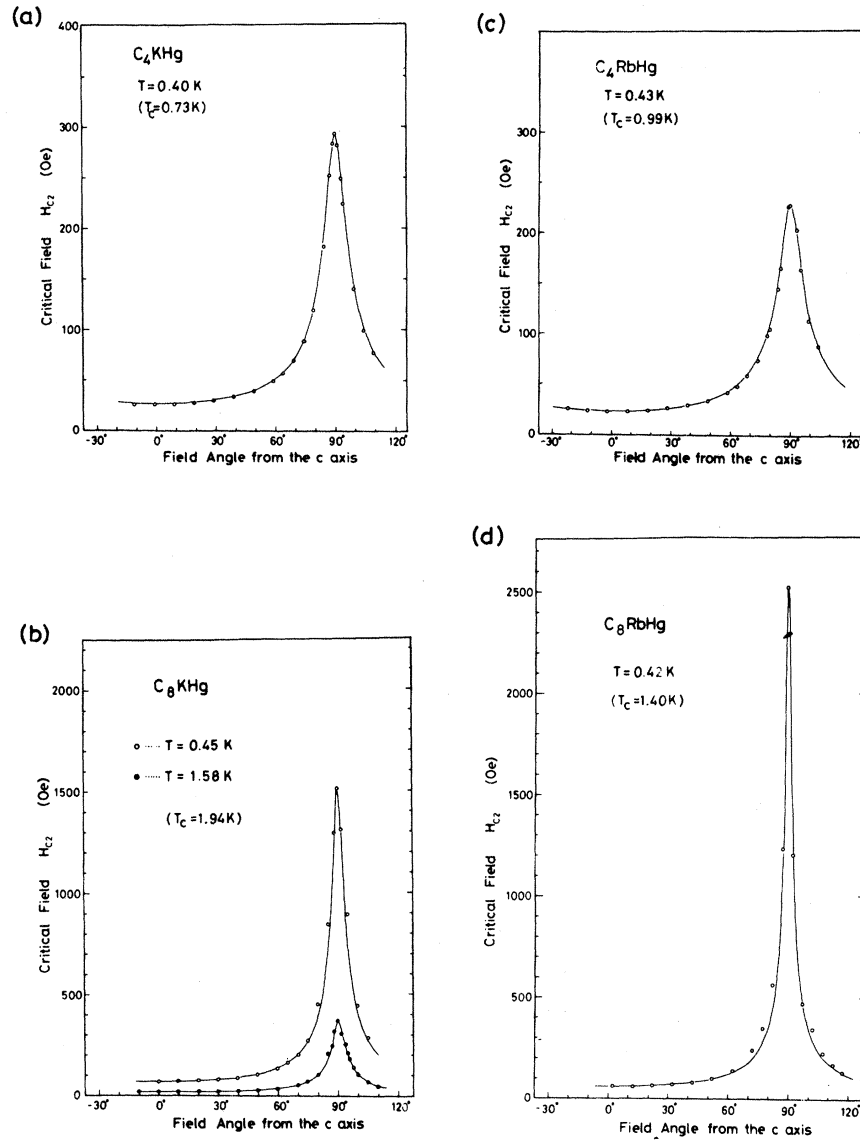


FIG. 3. Angular dependence of the critical field  $H_{c2}$  in the case of (a)  $C_4KHg$  (no. 3), (b)  $C_8KHg$  (no. 5), (c)  $C_4RbHg$  (no. 6), and (d)  $C_8RbHg$  (no. 9). The curves show the fitting of the angular dependence of the experimental points to the effective-mass model [Eq. (2)].

RbHg which are found to be isotropic type-II superconductors. It is noted that  $H_{c2}^{\parallel}$  at  $T=0$  of an amalgam GIC is smaller than  $H_{c2}(0)$  of the corresponding pristine amalgam, while  $H_{c2}^{\perp}(0)$  is larger than  $H_{c2}(0)$ .

By fitting Eqs. (5) and (6) to the linear region near  $T_c$ , we calculated the values of  $\xi_a(0)$  [ $=\xi(0)$ ] and  $\xi_c(0)$  [ $=\epsilon\xi(0)$ ]. Those values are summarized in Table I, together with other appropriate data. It should be noted that values of  $\xi_c(0)$  in Table I are those extrapolated from the GL region, and hence do not represent the true coherence length at abso-

lute zero, especially when  $H_{c2}^{\perp}$  has a positive curvature and the anisotropy ratio is no longer constant at lower temperatures, because of the superlinear temperature dependence of  $H_{c2}^{\perp}$ .

#### IV. DISCUSSION

Table I is a summary of experimental values of several quantities characterizing the superconductivity of amalgam GIC's. The data for  $C_8K$  by Koike *et al.*<sup>3</sup> are quoted for comparison. For

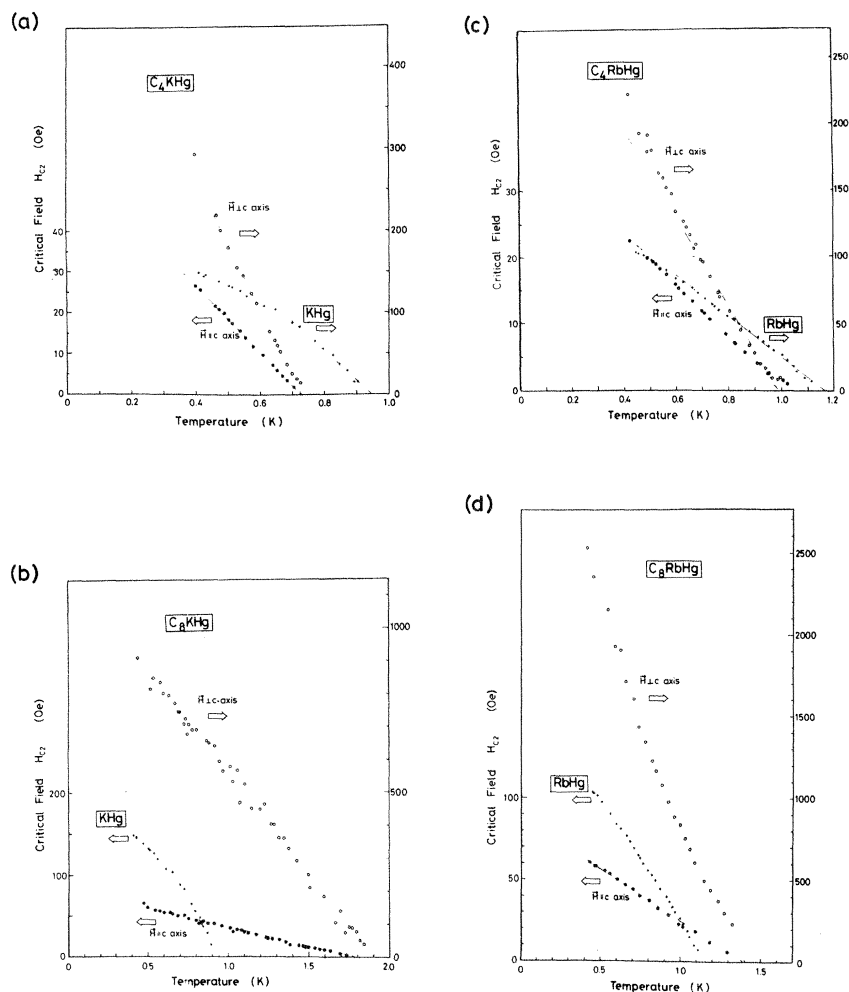


FIG. 4. Temperature dependence of the parallel and the perpendicular critical fields of (a)  $C_4KbHg$  (no. 3), (b)  $C_8KbHg$  (no. 4), (c)  $C_4RbHg$  (no. 6), and (d)  $C_8RbHg$  (no. 9). The critical fields of the pristine amalgams,  $KHg$  and  $RbHg$ , are also shown.

$C_8KbHg$ , the data of Koike and Tanuma<sup>8</sup> and Pendry *et al.*<sup>9</sup> are also shown for comparison.

First, it is seen that the values of  $T_c$  are in reasonable agreement for each compound. (The discussion on  $T_c$  will be given later in this section.) Secondly, with regard to the  $H_{c2}$  anisotropy, there is a large scatter in the experimental values, especially in the case of  $C_8KbHg$  and  $C_8RbHg$ . The origin of such discrepancies can be seen more clearly, if we look at the coherence length data. Namely, while the experimental values of the basal plane coherence length are in good agreement, those of the  $c$ -axis coherence length are quite sample dependent. The latter is mainly responsible for the scatter of the anisotropy ratio. The sample dependence of the  $c$ -axis coherence length is understandable because it is basically related to the elec-

tron conduction along the  $c$  axis which is quite defect-sensitive.

Figure 5 shows the stage dependence of the coherence lengths for the  $KHg$  and  $RbHg$  compounds. In this figure, stage zero denotes the pristine amalgams. It should be reminded here that a direct comparison between the amalgam GIC's and the pristine amalgams is only qualitative, because when intercalated the crystal structure of the amalgams is different from the pristine crystals.

In Fig. 5, it is seen that while the basal plane coherence length is only weakly stage dependent, the  $c$ -axis coherence length decreases rapidly with increasing stage. Thus, the stage-2 compounds have a larger anisotropy than the stage-1 compounds, and are more two dimensional. However, even for the stage-2 compounds, the  $c$ -axis coher-

TABLE I. Summary of the experimental data on the superconductivity of the alkali and alkali-amalgam GIC's.

Material	$I_c$ (Å)	Sample no.	$T_c$ (K)	$H_{c2}^{\perp}/H_{c2}^{\parallel}$ $=\epsilon^{-1}$	$-T_c \left[ \frac{dH_{c2}^{\parallel}}{dT} \right]_{T_c}$ (Oe)	$-T_c \left[ \frac{dH_{c2}^{\perp}}{dT} \right]_{T_c}$ (Oe)	$\xi_a(0)$ (Å)	$\xi_c(0)$ (Å)
C <sub>8</sub> K	5.40	L12 <sup>a</sup>	0.134	4.7	5.4	21.4	7800	2000
		P2 <sup>a</sup>	0.145	6.2	3.7	23.2	9400	1500
C <sub>4</sub> KHg	10.15	1	0.72	11.5	62.4	715	2300	200
		2	0.86	10.4	49.2	654	2600	200
		3	0.73	11.0	58.8	575	2400	240
C <sub>8</sub> KHg	13.50	4	1.90	15.5	81.2	1180	2000	140
		5	1.94	21.7	92.2	2050	1900	85
		A1 <sup>b</sup>	1.90	31	131	4370	1600	48
		A2 <sup>b</sup>	1.70	30	126	3910	1600	52
		c	1.90	40	96	3800	1800	45
C <sub>4</sub> RbHg	10.76	6	0.99	10.2	40.3	359	2900	320
		7 <sup>d</sup>	1.28	9.7	66.0	564	2200	261
C <sub>8</sub> RbHg	14.11	8	1.40	20.3	154	2700	1500	83
		9	1.40	41.3	87.9	2940	1900	58
			1.44					

<sup>a</sup>Reference 3.

<sup>b</sup>Reference 8.

<sup>c</sup>Reference 9.

<sup>d</sup>It is interesting that sample no. 7, which was found by the x-ray study to be a mixed crystal of C<sub>4</sub>RbHg and C<sub>8</sub>RbHg, showed a single transition at  $T_c = 1.28$  K, instead of a two-step transition corresponding to each stage.

ence length is still much longer than the  $c$ -axis repeat distance. This fact assures the validity of the application of the effective-mass model to the present case and indicates that even though it is highly anisotropic, the superconductivity of the amalgam GIC's is essentially three dimensional rather than two dimensional.

If we extrapolate the stage dependence of the  $c$ -axis coherence length as shown in Fig. 5, the extrapolated line crosses the line showing the weak stage dependence of the  $c$ -axis repeat distance at the stage 3. Therefore, if amalgam GIC's with stage higher than 3 are superconducting, they are expected to be two-dimensional superconductors. And the stage-3 amalgam GIC's, if superconducting, will provide an interesting situation of the crossover from a three-dimensional to a two-dimensional superconductivity.

Table II is a summary of the transition temperatures of the alkali-metal and alkali-metal - amalgam GIC's. The transition temperatures of the pristine amalgams are also shown for com-

parison. The data of the Debye temperatures  $\Theta_D$  and the electronic specific-heat coefficient  $\gamma$  are those reported by Alexander *et al.*<sup>10</sup> The Debye temperature  $\Theta_D$  characterizes the stiffness of phonons in a certain averaged sense. The electronic specific-heat coefficient is related to the electronic density of states at the Fermi level,  $N(0)$ , by

$$\gamma = \frac{\pi^2}{3} \kappa_B^2 (1 + \gamma) N(0), \quad (7)$$

where  $\gamma$  is the electron-phonon coupling parameter.

In the Bardeen-Cooper-Schrieffer (BCS) theory,<sup>16</sup>  $T_c$  is given by

$$T_c = 1.13 \Theta_D \exp[-1/N(0)V], \quad (8)$$

where  $V$  is the electron pairing potential. Using the data of  $T_c$  and  $\Theta_D$ , we obtain the values of  $N(0)V$  shown in the table. If we use McMillan's formula,<sup>17</sup>

$$T_c = \frac{\Theta_D}{1.45} \exp \left[ -\frac{1.04(1+\lambda)}{\lambda - \mu^*(1+0.62\lambda)} \right], \quad (9)$$

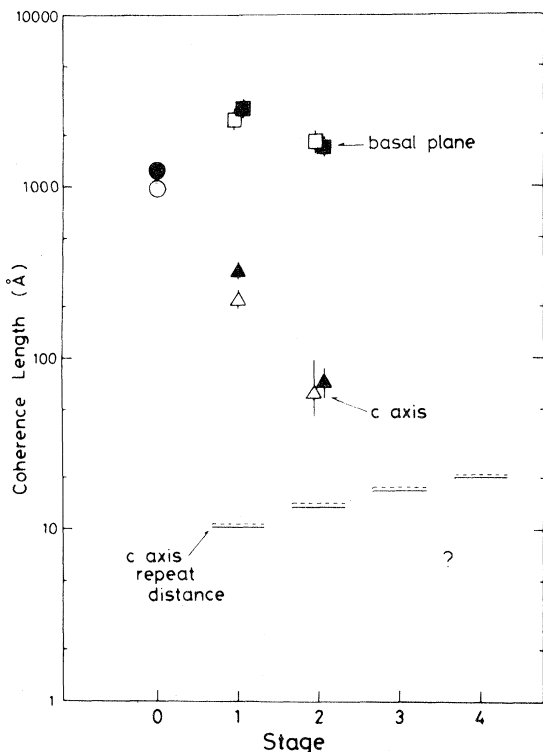


FIG. 5. Stage dependence of the basal plane and the *c*-axis coherence lengths. Stage zero denotes the pristine amalgam. The open symbols represent the KHg systems, and the solid symbols represent the RbHg systems. The solid and the broken lines drawn horizontally show the *c*-axis repeat distances for each stage of the KHg and RbHg GIC's. An extrapolation of the stage dependence of the *c*-axis coherence length is shown by the straight dotted line.

and a usually adopted assumption  $\mu^* = 0.1$ , we obtain the values of electron-phonon coupling constant  $\lambda$  shown in the last column of the table.

The electronic band structure of a GIC is such that it consists of graphite bands and intercalant bands. In the case of partial charge transfer ( $0 < f < 1$ ), there exist two carrier systems, i.e., carriers in the graphitic bands and those in the intercalant bands. This is the case in  $C_8K$ ,  $C_8Rb$ ,  $C_8Cs$ , and amalgam GIC's. In the case of  $C_6Li$  and higher-stage alkali-metal GIC's the charge transfer is unity so that the intercalant band is empty.

The question is then, which are responsible for superconductivity, electrons in the graphitic bands or electrons in the intercalant bands? From the arguments given below, we conclude that the latter are mainly contributing to the superconductivity.

The first point is the similarity of  $T_c$  between

the amalgam GIC's and their pristine amalgams. It is noted in Table II that  $T_c$  is of the order of 1 K both in the amalgam GIC's and in their pristine amalgams. The fact suggests that the superconductivity of the amalgam GIC's is essentially the same as that of the pristine amalgams.

The second point is the stage dependence of the anisotropy. We pointed out before that the stage-2 compounds have a larger anisotropy than the stage 1 (see Table I). This fact is consistent with the model that the intercalant electrons are superconducting, because in stage 2, two intercalant layers are separated by two carbon layers, while they are separated by one carbon layer in stage 1. This means that with respect to the intercalant bands, stage 2 is more two dimensional than stage 1. On the other hand, if the graphitic electrons are responsible for the superconductivity, the anisotropy should be, contrary to the experiment, decreased with increasing stage number, because with respect to the graphitic bands, higher stages are more three dimensional.

Thus, in the case of the amalgam GIC's, we conclude that the electrons in the intercalant bands are mainly contributing to the superconductivity. As for the alkali-metal GIC's, neither of the above arguments can be used, because pristine alkali metals are nonsuperconducting and superconductivity has not been found in higher stages. But in this case again, we speculate that the intercalant electrons are superconducting, because it explains why  $C_6Li$  does not show superconductivity despite a larger density of states at the Fermi level than  $C_8K$ . Namely, since charge transfer in the case of  $C_6Li$  is full ( $f = 1$ ), there exists no intercalant electrons.

Recently, Takada<sup>18</sup> developed a theory on the mechanism of the superconductivity of alkali-metal GIC's based on the model that the electrons in the alkali bands form Cooper pairs by a strong polar coupling with both optic and acoustic phonons. He calculated  $T_c$  as a function of charge transfer  $f$ , and obtained  $T_c \sim 0.1$  K for  $C_8K$  at the realistic value of  $f \sim 0.6$ . It may be concluded that in GIC's, the partial charge transfer ( $f < 1$ ) is essential for superconductivity.

The most puzzling thing about the superconductivity of the amalgam GIC's is the fact that the stage-2 compounds have higher  $T_c$  than the stage 1. By using McMillan's formula with an assumption  $\mu^* = 0.1$ , we obtained the values of the electron-phonon coupling constant  $\lambda$  shown in the last column of Table II. In this view, the higher  $T_c$  of the stage-2 compounds is attributed to larger



TABLE II. Comparison of the superconductivities of the alkali-metal and alkali-amalgam GIC's, and the pristine amalgams. The data of the Debye temperature  $\Theta_D$  and the electronic specific-heat coefficient  $\gamma$  are taken from Alexander *et al.* (Ref. 10).

Material	$T_c^a$ (K)	$\Theta_D^b$ (K)	$\gamma^b$ (mJ/mol deg <sup>2</sup> )	$N(0)V$	$\lambda$
C <sub>8</sub> K	0.14 <sup>c</sup>	374	0.75	0.13	0.30
C <sub>4</sub> KHg	0.73	269	0.95	0.17	0.38
C <sub>8</sub> KHg	1.90	260	0.2	0.20	0.46
KHg	0.94				
KHg <sub>2</sub>	1.20 <sup>d</sup>				
C <sub>3</sub> Rb	(< 0.09)	439	1.15		
C <sub>4</sub> RbHg	0.99				
C <sub>8</sub> RbHg	1.40	235	0.15	0.19	0.44
RbHg	1.17				

<sup>a</sup>The values for  $T_c$  given in the table represent an average over all samples measured.

<sup>b</sup>Reference 10.

<sup>c</sup>Reference 3.

<sup>d</sup>B. W. Roberts, J. Phys. Chem. Ref. Data 5, 661 (1976).

values of  $\lambda$ . Although we cannot do any better using the currently available data, such an analysis is certainly too naive. First, the Debye temperature obtained from the low-temperature specific heat is a measure of the phonon spectrum in such an averaged manner that low-lying phonon modes are more effective. These low-lying phonon modes do not necessarily correspond to the phonon modes most effective for electron pairing. Second, besides the intercalant electrons which, we believe, play the main role in superconductivity, there exist the graphitic electrons. For a quantitative estimation of  $T_c$ , the effect of Coulomb interaction and screening due to the graphitic electrons should be properly taken into account.

We conclude this section with a comparison of the present system with other layered superconductors. The layered superconductors so far investigated are mainly the following three kinds<sup>19</sup>: the Nb and Ta dichalcogenides, TaS<sub>2</sub> and NbS<sub>2</sub> intercalated with organic molecules, and MoS<sub>2</sub> intercalated with metal atoms. These materials provide a series of superconductors with varying degrees of two dimensionality. However, extra factors are present in this class of systems which sometimes make the experimental results rather complicated, i.e., the existence of polytypes and off-stoichiometry effects. With regard to this point, superconducting GIC's may provide a clearer sys-

tem.

The present system may be regarded as a hypothetical "layered" amalgam (though the actual KHg and RbHg are not layered materials) "intercalated" with carbon layers. As discussed in this section, the amalgam layers are superconducting, while the carbon layers are presumably not. In this view, the present system is in a sense analogous to the intercalated TaS<sub>2</sub> or NbS<sub>2</sub>, in which superconducting layers are separated by organic molecule layers. A more appropriate analogy may be the case of 4Hb-TaS<sub>2</sub>, which consists of alternating stackings of a trigonal prism layer and an octahedrally coordinated layer, where the former is superconducting while the latter is semiconducting.

With regard to the above analogy, the higher  $T_c$  of the stage-2 amalgam GIC's might be viewed as the transition-temperature enhancement associated with the carbon-layer intercalation. The behavior of  $T_c$  upon intercalation has been studied in the TaS<sub>2</sub> and NbS<sub>2</sub> systems. In the case of TaS<sub>2</sub>, the enhancement of  $T_c$  is observed upon intercalation, whereas a depression of  $T_c$  is observed in the case of NbS<sub>2</sub>. The  $T_c$  enhancement of the intercalated TaS<sub>2</sub> is usually explained in terms of the suppression of the charge density wave instability. The theoretical and experimental relationship between  $T_c$  and intercalation is an important point for further syntheses of layered superconductors.

## V. CONCLUSIONS

We have investigated the superconductivity of the stage-1 and -2 alkali-metal–amalgam GIC's ( $C_4KHg$ ,  $C_8KHg$ ,  $C_4RbHg$ ,  $C_8RbHg$ ) and of the pristine amalgams ( $KHg$ ,  $RbHg$ ). All of these four GIC's are type-II superconductors with transition temperatures of the order of 1 K, which are about the same as those of the corresponding pristine amalgams. The critical field anisotropy is larger for the stage-2 compounds whose  $c$ -axis repeat distance is larger than that of the stage 1. From these facts, we conclude that the electrons in the intercalant bands play the main role in the superconductivity of these materials. The angular dependence of the critical field is well explained by the effective-mass model, and the  $c$ -axis coherence length is much larger than the layer spacing. These observations indicate that these compounds are essentially three-dimensional superconductors rather than two-dimensional ones. The most in-

teresting feature is that stage 2 has a higher  $T_c$  than stage 1. To elucidate this problem, the investigation of stage-3 or higher-stage compounds, which we have not succeeded in synthesizing, will be very interesting.

## ACKNOWLEDGMENTS

The authors are grateful to Dr. A. W. Moore of Union Carbide Co. for donating high-quality HOPG samples, and to Professor W. Sasaki for letting them use the  $^3He$ -gas handling system. They also thank Professor H. Kamimura and Dr. Y. Takada and Dr. Y. Koike for helpful discussions and Professor M. S. Dresselhaus and Dr. G. Dresselhaus for critical reading of the manuscript. This work was supported in part by the Mitsubishi Foundation. One of the authors (Y. I.) appreciates the financial support by the Sakko-kai Foundation.

- 
- <sup>1</sup>N. B. Hannay, T. H. Geballe, B. T. Matthias, K. Andres, P. Schmidt, and D. MacNair, *Phys. Rev. Lett.* **14**, 225 (1965).
- <sup>2</sup>J. Poitrenaud, *Rev. Phys. Appl.* **5**, 275 (1970).
- <sup>3</sup>Y. Koike, H. Suematsu, K. Higuchi, and S. Tanuma, *Solid State Commun.*, **27**, 623 (1978); *J. Phys. Chem. Solids* **41**, 1111 (1980).
- <sup>4</sup>M. Kobayashi and I. Tsujikawa, *J. Phys. Soc. Jpn.* **46**, 1945 (1979).
- <sup>5</sup>Y. Koike, H. Suematsu, and S. Tanuma, private communication.
- <sup>6</sup>M. Kobayashi and I. Tsujikawa, private communication.
- <sup>7</sup>M. G. Alexander, D. P. Goshorn, D. Guerard, P. Lagrange, M. El Makrini, and D. G. Onn, *Syn. Met.* **2**, 203 (1980).
- <sup>8</sup>S. Tanuma, *Physica* **105B**, 486 (1981); Y. Koike and S. Tanuma, *J. Phys. Soc. Jpn.* **50**, 1964 (1981).
- <sup>9</sup>L. A. Pendry, R. W. Wachtman, F. L. Vogel, P. Lagrange, G. F. Furdin, M. El Makrini, and A. Herold, *Solid State Commun.* **38**, 677 (1981).
- <sup>10</sup>M. G. Alexander, D. P. Goshorn, D. Guerard, P. Lagrange, M. El Makrini, and D. G. Onn, *Solid State Commun.* **38**, 103 (1981).
- <sup>11</sup>P. Lagrange, M. El Makrini, D. Guerard, and A. Herold, *Physica* **99B**, 473 (1980); *Syn. Met.* **2**, 191 (1980).
- <sup>12</sup>R. C. Morris, R. V. Coleman, and R. Bhandar, *Phys. Rev. B* **5**, 895 (1972).
- <sup>13</sup>A. L. Fetter and P. C. Hohenberg, in *Superconductivity*, edited by R. D. Parks (Dekker, New York, 1969).
- <sup>14</sup>Among the papers on the superconductivity of the layered materials, there exists a confusion of the notation of  $H_{c2}^{\parallel}$  and  $H_{c2}^{\perp}$ . Throughout this paper, we use the notation in which "parallel" or "perpendicular" is always used by referring to the  $c$  axis of the crystal.
- <sup>15</sup>N. Toyota, H. Nakatsuji, K. Noto, A. Hoshi, N. Kobayashi, Y. Muto, and Y. Onodera, *J. Low Temp. Phys.* **25**, 485 (1976).
- <sup>16</sup>R. Meserve and B. B. Schwartz, in *Superconductivity*, edited by R. D. Parks (Dekker, New York, 1969).
- <sup>17</sup>W. L. McMillan, *Phys. Rev.* **167**, 331 (1968).
- <sup>18</sup>Y. Takada, *J. Phys. Soc. Jpn.* **51**, 63 (1982).
- <sup>19</sup>R. F. Frindt and D. J. Huntley, in *Physics and Chemistry of Materials with Layered Structures, Vol. 4, Optical and Electrical Properties*, edited by P. A. Lee (Reidel, Holland, 1976).